

SUPPORTING INFORMATION

Matrixes in MALDI Mass spectrometry – crystals of organic salts versus co-crystals of neutral polyfunctional carboxylic acids

Experimental

Physical Methods

The X-ray diffraction intensities were measured on a Bruker Smart X2S diffractometer, using micro 5 source Mo-K α radiation and employing the ω scan mode. The data were corrected for Lorentz and Polarization effects. An absorption correction based on multiple scanned reflections. The crystal structures were solved by direct methods using SHELXS-97 [1]. The crystal structures were refined by full-matrix least-squares refinement against F² [1]. Anisotropic displacement parameters were introduced for all non-hydrogen atoms. The hydrogen atoms attached to carbon were placed at 10 calculated positions and refined allowing them to ride on the parent carbon atom. The hydrogen atoms bound to nitrogen and the oxygen were constrained to the positions which were confirmed from the difference map and refined with the appropriate riding model. The experimental data are summarized in Table S1. The powder X-ray diffraction measurements were carried out on polycrystalline and/or glass samples. The XRD patterns were obtained using a Rigaku MiniFlex powder diffraction system, 15 equipped with a horizontal goniometer in the $\theta/2\text{-}\theta$ mode. The X-ray source was nickel-filtered K- α emission of copper (1.54056 Å). Samples were packed into an aluminium holder using a back-fill procedure and will be scanned over the range of 50 to 6 degrees 2- θ , at a scan rate of 0.5 degrees 2- θ /min. Using a data acquisition rate of 1 point per second, the scanning parameters equate to a step size 0 of 0.0084 degrees 2- θ . Calibration of each powder pattern will be effected using the characteristic 20 scattering peaks of aluminium at 44.738 and 38.472 degrees 2- θ .

HPLC-MS/MS measurements were made using TSQ 7000 instrument (Thermo Electron Corporation). Two mobile phase compositions were used: (A) 0.1 % v/v aqueous HCOOH and (B) 0.1 % v/v HCOOH in CH₃CN. Electrospray ionization (ESI) mass spectrometry. A triple quadrupole mass spectrometer (TSQ 7000 Thermo Electron, Dreieich, Germany) equipped with an ESI 2 source was 25 used and operated at the following conditions: capillary temperature 180°C; sheath gas 60 psi, corona

4.5 μ A and spray voltage 4.5 kV. Sample was dissolved in acetonitrile (1 mg ml⁻¹) and was injected in the ion source by an auto sampler (Surveyor) with a flow of pure acetonitrile (0.2 ml min⁻¹). Data processing was performed by Excalibur 1.4 software.

A standard LTQ Orbitrap XL instrument is used for the MALDI MS measurements, using the UV 5 laser source at 337 nm. An overall mass range of m/z 100–1000 is scanned simultaneously in the Orbitrap analyser. The samples are measures in solid state, using a variant of the spray technique of solution, containing the matrix and analyte compound. The solution of thus, obtained thin liquid films is fast evaporated to formation of the sample of matrix/matrix/analyte. The habitus of the crystals depends strongly of the crystallographic space system. Under these conditions however the obtained 10 polycrystalline samples are characterized with the relatively small crystal size, increasing the quality of the obtained spectra. The technique is also compared with the known solid-sample matrix techniques such as dried droplet, method of the crushed crystal, and over layered and sandwich method. The laser energy values are within 11.2–15.2 μ J. The numbers of averaged laser shots lies within 11–103, the MALDI flow rate values are within 25.2–23.2; the acquisition time is within 28.3–125.3 min, the 15 corresponding elapsed scan time range lies within 20.1 – 3.77 s, respectively.

The diffuse-reflectance spectra were measured on a PerkinElmer Lambda 750 in reflectance mode. The reflection spectra were automatically converted to absorbance spectra using Kubelka-Munk theory. The UV–VIS–NIR spectra between 190 and 1190 nm, using solvent acetonitrile (Uvasol, Merck product) at a concentration of 2.5.10⁻⁵ M in 0.921 cm quartz cells were recorded on Tecan 20 Safire Absorbance/Fluorescence XFluor 4 V 4.40 spectrophotometer.

Sample preparation for the MALDI-MS measurements

The natural alkaloid (**I**) is obtained according [2]. The matrixes were obtained, using the above preparation methods. For each of the obtained solid-samples for MALDI measurements, the crystallographic data, including the space groups and systems are compared using the powder X-ray

diffraction methods. This experiment is performed with a view to avoid formation of the polymorphs of the crystals (**1**)-(**4**) during the different matrix/matrix-analyte sample preparation techniques as well as controlling the obtaining of the salts with the natural alkaloids [4 in the main text]. As standard solvent for sample solutions, a mixture of methanol/water (1:1, v/v) was used. The MALDI 5 measurements of the different protonated forms of (**I**) in the matrixes in the samples, according the corresponding techniques are compared with the analysis of (**I**), using the standard dried droplet method in 2,5-dihydroxbenzoic acid (DHB), labeled as (**I**)-(**Sd**), respectively.

The dried droplet preparations were performed, using the 1 mol/l concentration of the of matrix solution plus and analyte solutions (10^{-4} - 10^{-3} M), both dissolved in methanol/water (1:1, v/v) solvent 10 mixtures. The obtained solutions were mixed on the MALDI target and dried by a gentle flow of air. The same analyte solutions were used for ESI-MS measurements, using however the acetonitrile:methanol solvent mixtures 1:1. The corresponding samples, obtained by this techniques are labeled as (**I**)-(**ia**), where i = (**1**)-(**4**), respectively. Under these conditions the powder X-ray diffraction method shows the formation of the crystals of the matrixes in large amounts as well as the crystals of 15 the salts of the natural alkaloids. The aggregations of the crystals (crystal sizes $> 5 \mu\text{m}$), were observed around the edge of the drop, thus leading to the inhomogeneous and irregular (random) distribution of the crystals on MALDI target.

The samples, using the crushed crystal method were prepared according the following procedure.

The preconcentrated solutions of the matrixes, obtained in solvent mixtures methanol:water under 20 heating at 70°C and reflux are cooled on air up to the r.t. thus prepared samples are slow evaporated in the presence of the nujol (Merck) with high viscosity (Fig. 1). The obtained crystals under the vacuum evaporation of the system, leads to formation of the single crystals with a relatively high crystal size (ca. up to 0.20 x 0.12 x 0.14 mm). It is important to note that under these conditions is avoided the formation of the crystal aggregates, allowing the application of the further fast evaporation technique

under the sandwich methods for deposition of the analyte on the matrix crystal surfaces. In this procedure, de facto the obtained data are comparable with those, using the dried droplet method in the presence of the DHB as matrix, since the neutral analytes are obtained. The corresponding samples are labeled as **(I)-(ib)**, where $i = (1)-(4)$, respectively

5 The electrospray method, consists of the electro spraying of the sample-analyte concentrated mixtures in solvent mixtures methanol:water 1:1 at the ratio 10⁴:1 matrix to analyte of the natural alkaloids from a high voltage of 3.1 kV, by the stainless-steel capillary onto a grounded standard metal plates advanced rubbing in one direction with the sand paper resulting to a channels with a diameter ca. 0.5 μm . Details are shown in [2]. This modification of the known technique [3] allows crystallization of 10 the matrix/matrix-analyte crystals in one direction consisting with the main crystallographic axes (Fig. S1), characterizing with a relatively small crystal size, under the aggregate dimensions of 1 μm (ca. 0.3–0.9 μm). Similar to the samples **(I)-(ia)**, the powder X-ray diffraction data show a formation of the polycrystalline samples of the matrixes and the crystals of salts of the natural alkaloids (Scheme 1), labeled as **(I)-(ic)**, respectively ($i = 1 - 4$).

15 It must taking into account that the pH values of the obtained matrix/analyte solutions in the dried droplet and the electrospray method could be change slightly during evaporation of the solvent, as a result of the strong acid in character of squaric acid, usually resulting to the full protonation process and cations formation with the N-alkyl and N_{py}-centres of organic compounds. A quantitative measure for the reliability of the peak assignments was expressed by the absolute deviation of measured and 20 calculated monoisotopic mass values. Direct integration approach depending of the MS method by a variation of the linear, and quadratic functions are tested, sowing the preference to the non-linear extrapolation. The highest r^2 values within 0.8972₃–0.932₁ are found at the higher concentrations, using ESI-MS method. The corresponding MLR and ANOVA data from the MALDI MSI method are

shown in Tables S4 and S5. The integration is performed in the continuous term of the dependences of the relative and absolute abundance.

Computational methods

Quantum chemistry

5 Quantum chemical calculations are performed with GAUSSIAN 09W and Dalton 2.0 program packages [4]. The geometries of isolated species were optimized, employing B3LYP method, Becke's three-parameter non-local exchange function with the correlation function of Lee, Yang and Parr, CAM-B3LYP and M06-2X, respectively. Molecular geometries were fully optimized by the force gradient method using Bernys' algorithm, using 6-31+G(d,p). For every structure the stationary points 10 found on the molecule potential energy hyper surfaces were characterized using standard analytical harmonic vibrational analysis. The UV spectra in methanol were predicted, using the experimental geometries by the crystallographic experiment, by TDDFT method, utilizing primarily the polarizable continuum model (PCM). The calculations are utilized by large "correlation consistent" basis sets aug-cc-pVDZ and aug-cc-pVTZ [4].

15 Chemometrics

The experimental and theoretical spectroscopic patterns were processed by R4Cal OpenOffice STATISTICS for Windows 7 [5] program package. Baseline corrections and curve-fitting procedures were applied. The baseline was calculated using the standard linear equation. The curve-fitting nonlinear procedure was applied. In the case of the Levenberg-Marquardt method, the merit equation 20 used is χ^2 the equation. The final solution is found when a minimum in the reduced χ^2 equation is reached. It is a statistical measure of "goodness-of-fit", inversely proportional to the known variance of the data set. The statistical significance of each regression coefficient was checked by the use of t-test (calculation of the number of significance using data from the experimental error, usually higher than 0.100). The model fit was determined by F-test. The obtained dependences from the primary ionization

MALDI mechanism during the laser pulses ionization are evaluated by the fast Fourier Transform (FFT) method [5].

The Fourier methods appear especially informative to evaluate and analyses the non-linearity of the MALDI MS experiments. Nevertheless the Fourier analysis is suited for the liner systems, all 5 experimental systems however are somewhat non-linear such as laser sources, describing as working in heterodyning regime, i.e. by the Fourier analysis is possible to reorganized the artifacts of the non-linear responses.

Levenberg-Marquardt method, provide a numerical solutions in the case of problematic minimizations of the non-linear or least-square curve-fitting functions over the space of the parameters of the 10 function. It is important to note that the method find only the local minimum, which is nit obligatory coincide with the global minimum. The application of the is in the least squares curve fitting problem: given a set of n-empirical datum pairs of independent and dependent variables, (x_i, y_i) , optimize the parameters β of the model curve $f(x, \beta)$ so that the sum of the squares of the deviations becomes minimal:

$$15 \quad S(\beta) = \sum_{i=1}^n [y_i - f(x_i, \beta)]^2$$

The method is an iterative procedure, where to start the minimization has to provide an initial guess for the parameter vector β . In cases with only one minimum, an uninformed standard guess will work fine. In the cases of the in cases with series of minima, the algorithm converges only if the initial guess is already somewhat close to the final solution. In each iteration step, the parameter vector, β is replaced 20 by a new estimate $\beta + \delta$. To determine δ , small deviation, the functions $f(x_i, \beta + \delta)$ are approximated by their linearization where:

$$f(x_i, \beta + \delta) \approx f(x_i, \beta) + J_i \delta; J_i = \frac{\partial f(x_i, \beta)}{\partial \beta}$$

The J_i is the row-vector in this case of f with respect to β .

An example of the algorithm could be shown, using the absolute intensity versus the scan number in the MALDI-MSI method. The best fitting is obtained (red solid-line, using the 2000 iterations. The χ^2 of 1.10^{-4} is obtained (Fig. S2).

The perform Multiple Linear Regression (MLR) analysis (Tables S4 and S5), highlighted the 5 independent variable columns of data sets. The obtained value t-values for testing if the parameter equals zero, where $t = \text{the parameter estimate}/\text{standard error of the estimate}$; p-value: A partial F-test is computed for each of the independent variables still in the equation. $F \text{ statistic} = [\text{RSS}^2 - \text{RSS}^1]/\text{ESD}^2$, where $\text{RSS}^1 = \text{the residual sum of squares with all variables that are presently in the equation}$; $\text{RSS}^2 = \text{the residual sum of squares with one of the variables removed}$, and $\text{ESD}^1 = \text{the Mean Square for Error}$ 10 with all variables. The Analysis of Variance (ANOVA) for MLR, includes Levene's test and the Brown-Forsythe test for equal variance. It is preformed to test whether or not two or more populations have the same mean. The main analysis is based on the assumption that the data sets follow a normal distribution with constant variance. The null hypothesis is that the means of all selected data sets are equal. The alternative hypothesis is that the means of one or more selected data sets are different. The 15 basic equations are $\text{SST} = \text{SSM} + \text{SSE}$, where SS is notation for sum of squares and T, M, and E are notation for total, model, and error, respectively. The square of the sample correlation is equal to the ratio of the model sum of squares to the total sum of squares: $r^2 = \text{SSM}/\text{SST}$. The interpretation of r^2 is to explain the fraction of variability in the data explained by the regression model.

20

References*

*The reference numbering in the supporting information file was independent from this in the main text of the manuscript

- [1] (a) G.M. Sheldrick *Acta Cryst.* 2008, **A64**, 112; (b) R. Blessing *Acta Cryst.* 1995, **A51**, 33; (c) A. 25 Spek, *J. Appl. Cryst.* 2003, **36**, 7; (d) L. Farrugia, *J. Appl. Cryst.* 1997, **30**, 565.

- [2] (a) F. Xiang, R. Beavis, *Rapid Commun. Mass Spectrometry*, 1994, **8**, 199; (b) O. Vorm, P. Roepstorff, M. Mann, *Anal. Chem.* 1999, **66**, 199; (c) Y. Dai, R. Wittal, L. Li, *Anal. Chem.* 1994, **66**, 3281; (d) L. Li, R. Golding, R. Wittal, *J. Am. Chem. Soc.* 1996, **118**, 11662; (e) J. Zheng, N. Li, M. Ridyard, H. Dai, S. Robbins, L. Li, *J. Proteom. Res.* 2005, **4**, 1709; (f) S. Cohen, B. Chait, *Anal. Chem.* 1996, **68**, 31 ; (g) R. Hensel, R. Kinng, K. Owens, *Rapid. Commun. Mass Spectrom.* 1997, **11**, 1785 ; (h) J. Axelsson, A. Hoberg, C. Waterson, R. Myatt, G. Chield, J. Varney, D. Haddleton, J. Derrick, *Rapid. Commun. Mass Spectrom.* 1997, **11**, 209; (i) R. Caprioli, T. Farmer, J. Gile, *Anal. Chem.* 1997, **69**, 4751.
- [3] (a) B. Ivanova, M. Spiteller, *Struct. Chem.* 2010, **21**, 989; (b) B. Koleva, T. Kolev, R. Seidel, M. Spiteller, H. Mayer-Figge, W. Sheldrick, *J. Phys. Chem. A* 2009, **113**, 3088; (c) B. Ivanova, M. Spiteller, *J. Phys. Chem. A* 2010, **114**, 5099; (d) B. Ivanova, M. Spiteller, *Cryst. Growth Des.* 2010, **10**, 2470; (e) B. Ivanova, M. Spiteller, *Spectrochim. Acta* 2010, **77**, 849; (e) B. Ivanova, M. Spiteller, *Polyhedron* 2011, **30**, 241; (f) B. Koleva, T. Kolev, V. Simeonov, T. Spassov, M. Spiteller, *J. Inclus. Phenomen.* 2008, **61**, 319; (g) M. Lamshoeft, J. Storp, B. Ivanova, M. Spiteller, *Polyhedron* 2011, **30**, 15 2564.
- [4] (a) M. Frisch, G. Trucks, Schlegel, H. Scuseria, G. Robb, M. Cheeseman, J. Zakrzewski, V. Montgomery Jr., J. Stratmann, R. Burant, J. Dapprich, S.; Millam, J. Daniels, A. Kudin, K. Strain, M. Farkas, Ö.; Tomasi, J.; Barone, V.; Cossi, M.; Cammi, R.; Mennucci, B.; Pomelli, C.; Adamo, C.; Clifford, S.; Ochterski, J.; Petersson, G. Ayala, P. Cui, Q.; Morokuma, K.; Salvador, P.; Dannenberg, J. Malick, D. Rabuck, A. Raghavachari, K.; Foresman, J. Cioslowski, J.; Ortiz, J. Baboul, A. G.; Stefanov, B. Liu, G.; Liashenko, A.; Piskorz, P.; Komáromi, I.; Gomperts, R.; Martin, R. Fox, D. Keith, T.; Al-Laham, M. Peng, C. Nanayakkara, A.; Challacombe, M.; Gill, P. Johnson, B.; Chen, W.; Wong, M. Andres, J. Gonzalez, C.; Head-Gordon, M.; Replogle, E. Pople, J. Gaussian 98, Gaussian, Inc., Pittsburgh, PA, 2009; (b) Dalton 2.0 Program Package

- <http://www.kjemi.uio.no/software/dalton/dalton.html>; (c) GausView03,
<http://www.softwarecientifico.com/paginas/gaussian.htm>; (d) Y. Zhao, D. Truhlar, *Accts. Chem. Res.* 2008, **41**, 157; (e) N. Schultz, Y. Zhao, D. Truhlar, *J. Comput. Chem.* 2008, **29**, 185; (f) Y. Zhao, D. Truhlar, *Theor. Chem. Acc.* 2008, **120**, 215; (g) D. Woon, T. Dunning, *J. Chem. Phys.* 1993, **98**, 1358; (h) J. Foresman, M. Head-Gordon, J. Pople, M. Frisch, *J. Phys. Chem.* 1992, **96**, 135; (i) K. Wiberg, C. Hadad, J. Foresman, W. Chupka, *J. Phys. Chem.* 1992, **96**, 10756; (j) R. Bauernschmitt, R. Ahlrichs, *Chem. Phys. Lett.* 1996, **256**, 454; (k) R. Stratmann, G. Scuseria, M. Frisch, *J. Chem. Phys.*, 1996, **109**, 8218; (l) B. Ivanova, M. Spiteller, *Biopolymers* 2010, **93**, 727; (m) B. Ivanova, M. Spiteller, *J. Mol. Struct.* 2011 doi:10.1016/j.molstruc.2011.06.043; (n) M. Lamshoft, B. Ivanova, M. Spiteller, *Talanta*, 10 2011, 10.1016/j.talanta.2011.08.008.
- [5] (a) <http://de.openoffice.org/>; (b) P. Stephens, D. McCann, J. Cheeseman, M. Frisch, *Chirality* 2005, **17**, S52; (c) P. Stephens, F. Devlin, J. Cheeseman, M. Frisch, O. Bortolini, P. Besse, *Chirality* 2003, **15**, S57; (d) A. Yildiz, P. Selvin, *Accts. Chem. Res.* 2005, **38**, 574; (e) E. Wyrzykiewicz, W. Boczon, B. Koziol, *J. Mass Spectrom.* 2000, **35**, 1271; (f) M. Lamshoft, J. Storp, B. Ivanova, M. Spiteller, *Polyhedron* 2011, **30**, 2564; (g) K. Levenberg, *Quarter. Appl. Math.* 1944, **2**, 164; (h) D. Marquardt, *SIAM J. Appl. Math.* 1953, **11**, 431; (h) A. Girard *Rev. Opt.* 1958, **37**, 225; (i) A. Marshall, F. Verdun, Fourier Transforms in NMR, Optical and Mass Spectrometry, Elsevier Sci. Publish. Company Inc., USA, 1990.

Table S1. Crystallographic and refinement data

	(1)	(2)	(3)	(4)	M1	M2	M3
Empirical formula	C ₁₀ H ₈ N ₂ O ₅	C ₁₀ H ₈ N ₂ O ₅	C ₈ H ₇ N ₂ O ₃	C ₁₆ H ₁₁ NO ₅	C ₂₄ H ₃₄ C ₁₀ N ₂ O ₈	C ₁₄ H ₂₁ N ₂ O ₄	C ₈ H ₈ O ₃
M _r	236.18	236.18	179.16	297.26	478.53	281.33	152.14
Crystal size	0.13×0.09×0.08	0.33×0.18×0.17	0.47×0.31×0.21	0.22×0.20×0.08	0.14×0.10×0.08	0.35×0.26×0.17	0.48×0.25×0.16
Crystal system	Monoclinic	Monoclinic	Monoclinic	Monoclinic	Orthorhombic	Monoclinic	Orthorhombic
Space group	P2 ₁ /c	P2 ₁ /n	C2/c	P2 ₁ /c	P2 ₁ 2 ₁ 2 ₁	P21/n	Pbc _a
T [K]	199(2)	198(2)	293(2)	300(2)	199(2)	200(2)	198(2)
λ [Å]	0.71073	0.71073	0.71073	0.71073	0.71073	0.71073	0.71073
<i>a</i> [Å]	4.1827(8)	3.7755(11)	21.047(6)	15.7822(18)	7.711(3)	11.024(4)	9.9537(15)
<i>b</i> [Å]	11.899(2)	27.441(10)	8.368(2)	7.2392(9)	12.974(6)	9.290(3)	9.6632(15)
<i>c</i> [Å]	20.394(4)	9.687(3)	9.364(2)	12.5086(17)	23.865(11)	29.254(11)	16.173(3)
α [°]	90	90	90	90	90	90	90
β [°]	93.148(7)	100.495(11)	101.972(8)	106.033(4)	90	98.054(12)	90
γ [°]	90	90	90	90	90	90	90
<i>V</i> [Å ³]	1013.5(4)	8(6)	1613.2(7)	1373.5(3)	2387.3(19)	2966.4(19)	1555.6(4)
<i>Z</i>	4	4	8	4	4	8	8
μ [mm ⁻¹]	0.127	0.130	0.116	0.109	0.093	0.100	
ρ _{calc} [mg m ⁻³]	1.548	1.590	1.475	1.437	1.331	1.260	1.299
2θ [°]	25.07	21.72	25.16	25.05	19.21	25.56	25.10
Reflections collected	6255	4445	4877	8370	12494	17504	8941
Goodness-of-fit on <i>F</i> ²	1.102	0.987	0.687	0.955	1.032	0.891	0.796
<i>R</i> ₁ [$\text{I} > 2\sigma(\text{I})$]	0.0432	0.0477	0.0360	0.0392	0.1047	0.0935	0.0410
CCDC	770383	770384	770387	760138			

Table S2. Hydrogen bonds in the crystals of **(1)-(4)**; bond lengths [Å]

	(1)	(2)	(3)	(4)
$\text{O}_{(\text{Sq})}\text{OH} \cdots \text{O}_{(\text{Sq})}$	2.500	2.507	2.622	2.507(2)
$\text{N}^+\text{H} \cdots \text{O}$	2.737	2.949, 2.810	2.769	2.645(2)
$\text{OH} \cdots \text{O}$	2.669	2.769	2.585	

Table S3. Theoretical and experimental electronic absorption spectra of the crystals of (1)-(4) in methanol, calculated, using the unit cell contents of two neighbouring cells.

	(1) Theoretical	(2) Experimental	(2) Theoretical	(3) Experimental	(3) Theoretical	(4) Experimental	Theoretical	Experimental
244			212 230	210 227	210 228 240	210 228 236	210 228	210 228
			241				238 262 281	238 262 281
285			284	305	292 330	335		
			285					

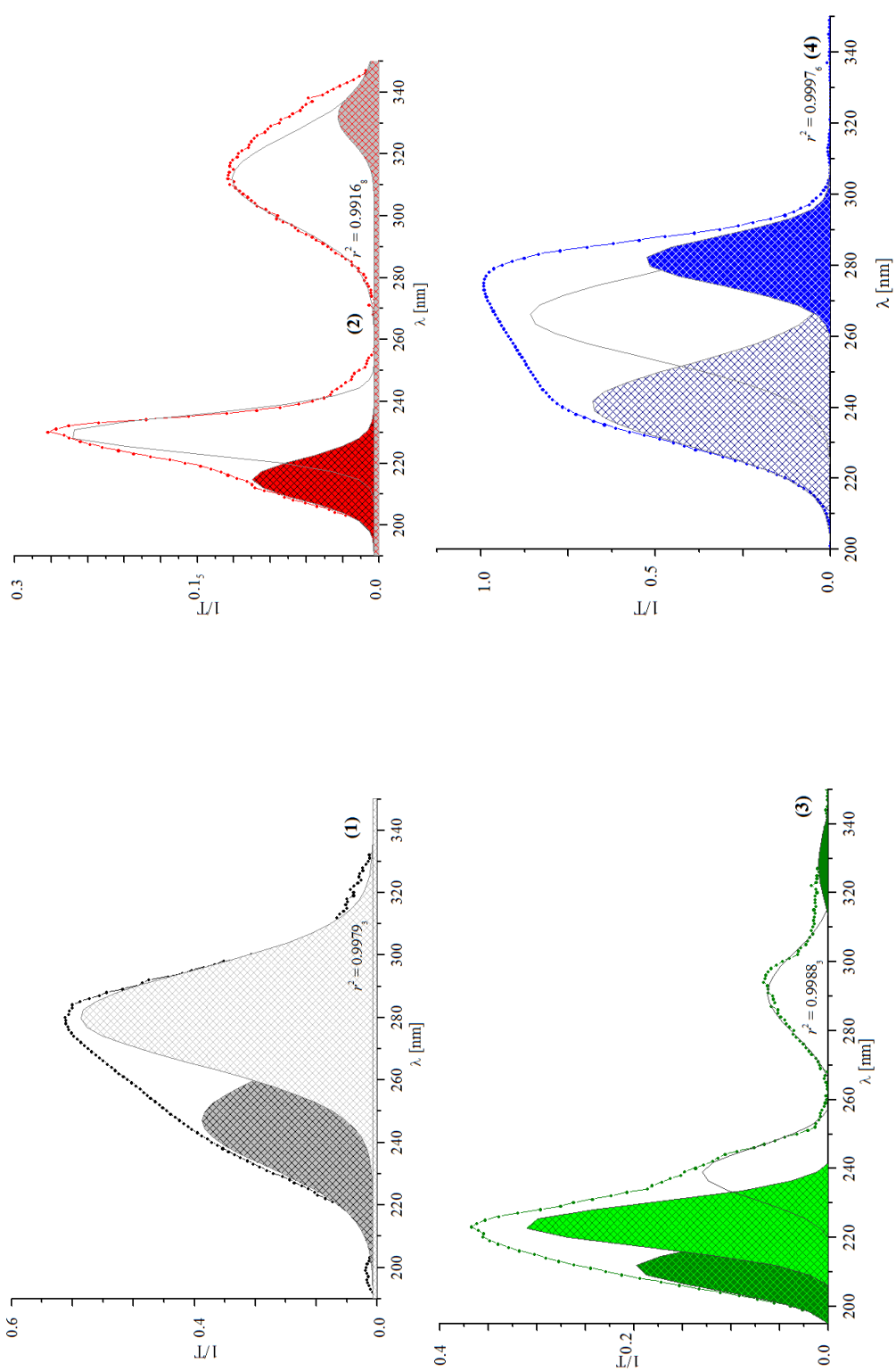


Figure S1. Electronic transmission (T , %) and absorption ($1/T$) spectra of (1)-(4) in methanol at $2.4 \cdot 10^{-4}$ mol/L concentration and 0.998_3 cm quartz cell; curve-fitted spectroscopic patterns after the baseline correction method, by non-linear multi peak Gaussian function; A - total area under the curve from the baseline centre of the peak; w^2 "sigma", approximately 0.849 the FWHM; $w/2$ - is the standard deviation, respectively.

5

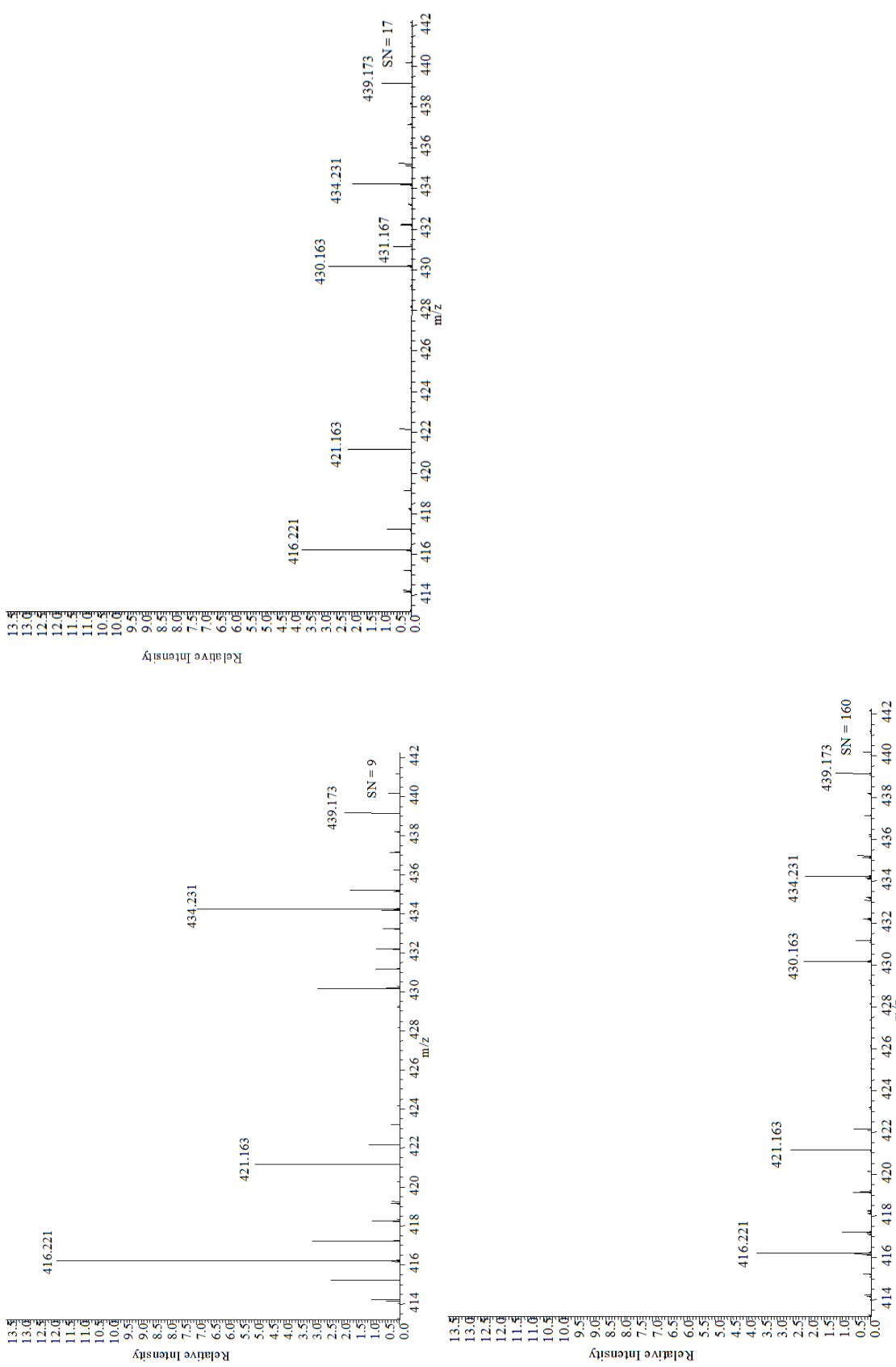
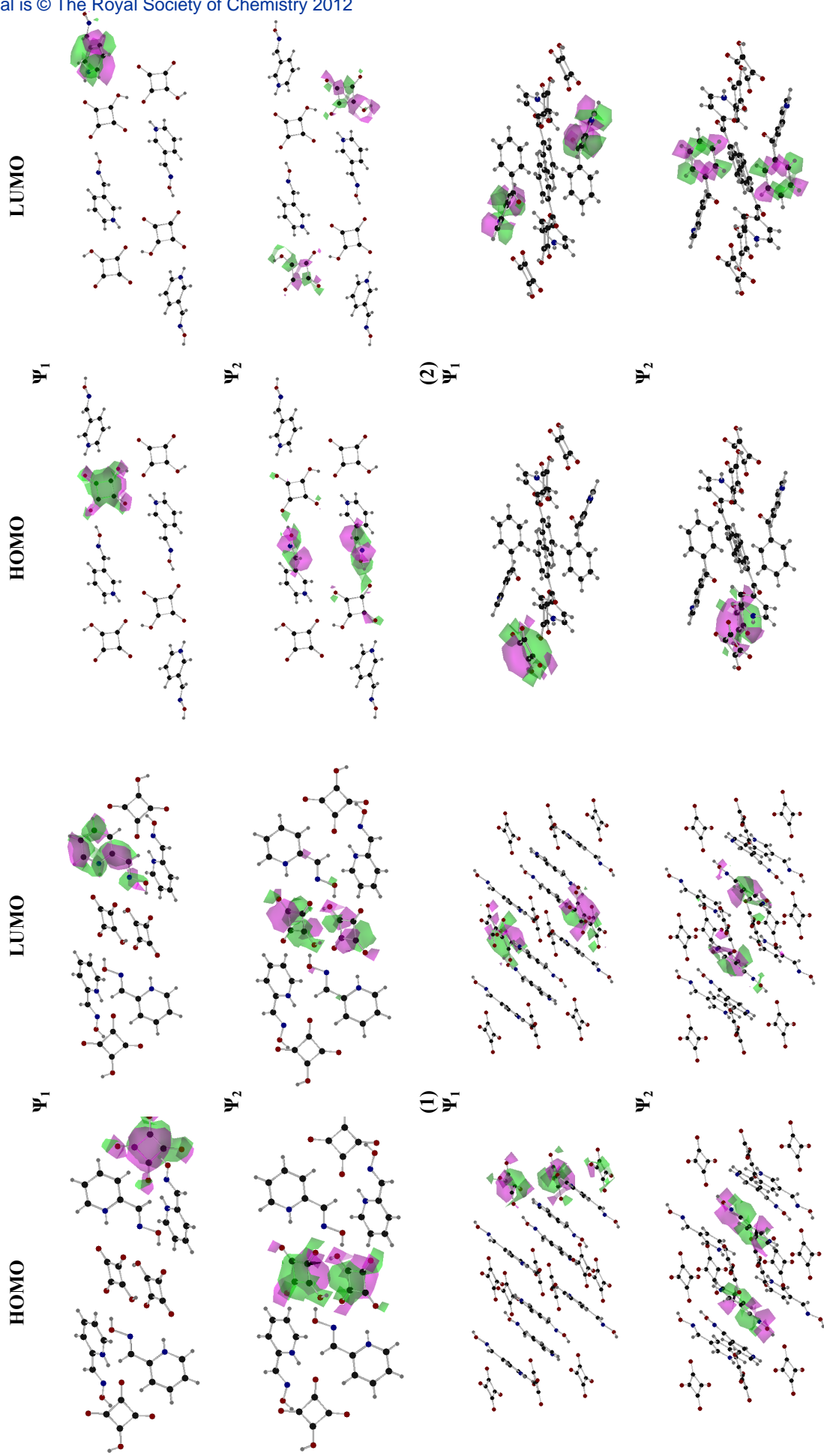


Figure S2. Mass spectra at the location of the surface for the systems (1)-(1) – (4)-(1) in the different scan areas, presented as corresponding SN.

Table S4. Quantitative parameters as SN – scan number (areas shown in Fig. 5); integrated A - Area, obtained P-peak position, W-width, and H – Height values; The calculated A^i/A^j values for the different peaks in the frame of one SN area.												
		439.173			416.221			434.231				
S	A	P	W	H	A	P	W	H	A	P	W	H
N												
9	36047.862	439.173	1.976	36367.848	8154.775	416.221	0.062	262497.366	5033.203	434.231	0.065	153586.016
17	345096.883	439.173	1.002	696053.072	123375.053	416.221	0.097	2.561.10 ⁶	14390.194	434.231	0.02	1.436.10 ⁶
160	15932.675	439.173	0.041	784484.264	59704.748	416.221	0.046	2.604.10 ⁶	1648.882	434.174	0.038	87799.548
188	47978.417	439.173	0.127	753383.488	98792.032	416.221	0.049	4.032.10 ⁶	39106.186	434.231	0.032	2.436.10 ⁶
280	23542.290	439.173	0.021	2.238.10 ⁶	1.178.10 ⁶	416.221	0.887	2.537.10 ⁶	537071.262	434.231	0.886	1.206.10 ⁶
S	A	P	W	H	A	P	W	H	A	P	W	H
N												
9	106583.189	476.218	1.028	20991.4216	3746.555	520.255	1.003	7526.578				
17	1.509.10 ⁶	476.219	1.001	3.028.10 ⁶	89025.591	520.255	0.959	18231.8787				
160	630397.482	476.219	0.999	1.262.10 ⁶	54145.260	520.255	0.959	11481.0791				
188	42585.502	476.219	0.041	2.073.10 ⁶	113399.563	520.255	0.965	240526.184				
280	272376.168	476.219	0.829	659904.430	1284.150	520.255	0.965	11462.796				
S	A	P	W	H	A	P	W	H	A	P	W	H
N												
9	21501.216	262.126	0.81	53195.378	3464.550	233.148	0.908	7562.144	3351.399	136.092	7.282	7562.144
17	122125.709	262.126	0.012	2.031.10 ⁷	1.281.10 ⁶	233.147	0.784	3.267.10 ⁶	81071.716	136.092	0.188	861435.813
160	127143.899	262.126	0.014	1.812.10 ⁷	664714.265	233.147	0.784	1.695.10 ⁶	345913.617	136.092	1.002	683202.8
188	113138.55	262.126	0.012	1.885.10 ⁷	1.225.10 ⁶	233.147	0.955	2.579.10 ⁶	442059.318	136.092	1.031	857473.0
280	74961.434	262.126	0.011	1.349.10 ⁷	723734.910	233.147	0.915	1.571.10 ⁶	371958.359	136.092	1.04	716407.845
S	A	P	W	H	A	P	W	H	A	P	W	H
N												
9	$A^{439.173}/A^{416.221}$	$A^{439.173}/A^{476.219}$	$A^{439.173}/A^{520.255}$	$A^{439.173}/A^{520.225}$	$A^{439.173}/A^{262.126}$	$A^{439.173}/A^{233.147}$	$A^{439.173}/A^{136.092}$	$A^{439.173}/A^{136.092}$	$A^{416.221}/A^{434.231}$	$A^{416.221}/A^{476.219}$		
17	4.421	7.162	0.338	9.622	1.677	10.404	10.756	1.620		21.176		
160	2.797	23.981	$\sim 0 (10^{-6})$	3.876	2.826	~ 0	4.257	8.574		~ 0		
188	0.267	~ 0	0.025	0.295	0.126	0.034	0.046	36.209		0.095		
280	0.486	0.487	1.127	0.423	0.424	~ 0	0.109	2.526		2.319		
S	A	$A^{416.221}/A^{520.255}$	$A^{416.221}/A^{262.126}$	$A^{416.221}/A^{233.147}$	$A^{416.221}/A^{476.219}$	$A^{434.231}/A^{520.255}$	$A^{434.231}/A^{262.126}$	$A^{434.231}/A^{233.147}$	$A^{434.231}/A^{136.092}$	$A^{416.221}/A^{476.219}$		
N												
9	2.717	0.379	0.011	2.433	0.047	1.243	0.234	1.453		1.501		
17	1.386	1.010	~ 0	1.521	~ 0	0.61	0.118	~ 0		0.177		
160	1.102	0.469	0.089	0.173	1.426	0.031	0.012	0.002		0.005		
188	0.872	0.873	~ 0	0.224	0.918	0.345	0.346	~ 0		0.088		
280	~ 0	~ 0	~ 0	1.971	0.742	7.164	0.741	1.443				
S	A	$A^{476.219}/A^{520.255}$	$A^{476.219}/A^{262.126}$	$A^{476.219}/A^{233.147}$	$A^{476.219}/A^{136.092}$	$A^{520.255}/A^{262.126}$	$A^{520.255}/A^{136.092}$	$A^{262.126}/A^{233.147}$	$A^{262.126}/A^{136.092}$	$A^{262.126}/A^{476.219}$		
N												
9	28.448	4.957	30.764	31.803	0.175	1.082	1.118	6.206		6.416		
17	16.951	12.563	1.177	18.614	0.729	~ 0	1.098	~ 0		1.506		
160	11.643	7.865	0.948	1.953	0.426	0.082	0.157	0.191		0.367		
188	0.375	1.0	~ 0	0.096	1.002	0.256	~ 0	0.003		0.256		
280	212.106	3.633	0.376	0.732	0.017	0.002	0.017	0.104		0.202		

Table S5. Multiple Regression Analysis and ANOVA test the data in Table 1 towards “A”.

	V Value	Std. Error	t-Value	Prob (> t)	r ²	ESD	df	SS	MS	F Statistic	Prob (> F)
A ^{439.173}											
16072.760	14968.9332	1.0737	0.3953	0.9851	24352.4314	Model	2	7.8398.10 ¹⁰	3.9199.10 ⁹	66.0986	0.0149
18.6642	33.3309	0.5599	0.6319			Error	2	1.1860.10 ⁹	5.9304.10 ⁸		
-17.7147	33.3489	-0.5311	0.6483			Total	4	7.9584.10 ¹⁰			
A ^{434.231}											
14923.4711	36710.7500	0.4065	0.6984	0.8047	86772.7331	Model	2	1.8617.10 ¹¹	9.3086.10 ¹⁰	12.3628	0.0075
29.4279	111.0082	0.2651	0.7998			Error	6	4.5177.10 ¹⁰	7.529510 ⁹		
-28.645	111.0252	-0.2580	0.8050			Total	8	2.3134.10 ¹¹			
A ^{136.092}											
35474.17879	47229.3771	0.7511	0.481	0.7974	87550.4863	Model	2	1.810410 ¹¹	9.052.10 ⁹	11.8094	0.0083
62.03754	116.4968	0.5325	0.6135			Error	6	4.599110 ¹⁰	7.6651.10 ⁹		
-61.2659	116.5504	-0.5257	0.6180			Total	8	2.270310 ¹¹			



Scheme S1. HOMO-LUMO MO gaps of the crystals (1)-(4), obtained using the crystallographic data for the two neighbouring unit cell content

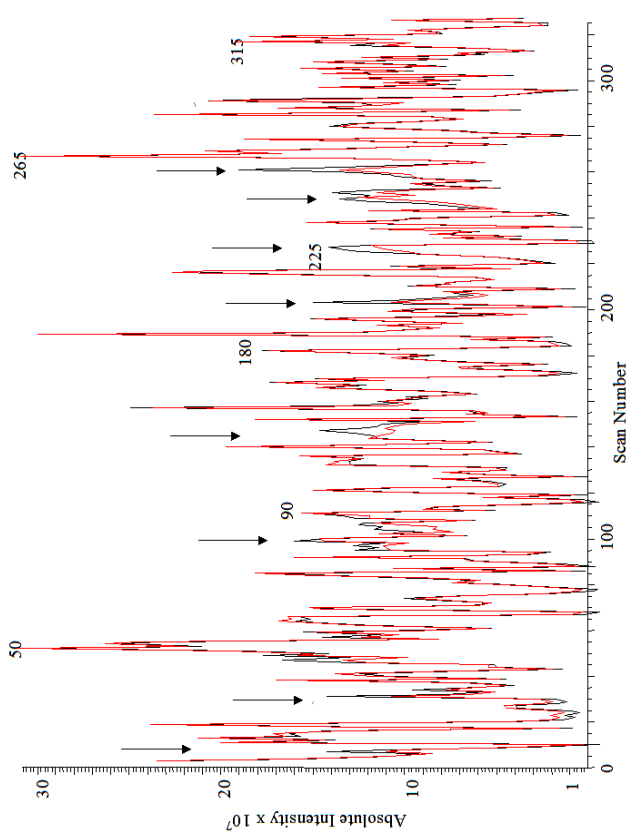


Figure S3. The Absolute intensity vs. the scan number, obtained from the MALDI MS experiment for the system (I)-(1) (black solid-line). The Levenberg–Marquardt algorithm implemented as the least square function is shown as red-solid-line. The corresponding deviations are shown as arrows.